

Refereed Proceedings

*The 12th International Conference on
Fluidization - New Horizons in Fluidization
Engineering*

Engineering Conferences International

Year 2007

Comparison of Simulated and Measured
Flow Patterns: Solid and Gas Mixing in
a 2D Turbulent Fluidized Bed

Ulla Ojaniemi*

Sirpa Kallio[†]

Alf Hermanson[‡]

Mikko Manninen**

Maiju Seppälä^{††}

Veikko Taivassalo^{‡‡}

*VTT, Finland, ulla.ojaniemi@vtt.fi

[†]Åbo Akademi University, Finland

[‡]Åbo Akademi University, Finland

**VTT, Finland

^{††}VTT, Finland

^{‡‡}VTT, Finland

This paper is posted at ECI Digital Archives.

http://dc.engconfintl.org/fluidization_xii/89

Ojaniemi et al.: Solid and Gas Mixing in a 2D Turbulent Fluidized Bed

Comparison of simulated and measured flow patterns: Solid and gas mixing in a 2D turbulent fluidized bed

Ulla Ojaniemi⁺, Sirpa Kallio^{*}, Alf Hermanson^{*},

Mikko Manninen⁺, Maiju Seppälä⁺, Veikko Taivassalo⁺

⁺Åbo Akademi Univ., Heat Engineering lab., Piispank. 8, FI-20500 Turku, Finland

^{*}VTT, P.O.Box 1000, FI-02044 VTT, Finland

ABSTRACT

Results from experiments done in a 2D turbulent fluidized bed cold model are presented. Experiments were conducted to study flow patterns, particle mixing in the bed and spreading of gas blown from one side into the bed. 2D simulations of the experiments were carried out using the Eulerian multiphase models of the Fluent and MFIX CFD softwares.

INTRODUCTION

CFD modeling of fluidized beds is nowadays commonly performed applying the kinetic theory model of granular flow and a transient description (e.g. [1,2](#)). The models for granular multiphase flows presented in literature predict reasonably correctly the overall behavior of fluidized beds, especially stationary beds. However, more validation studies are necessary to test and improve the reliability of the modeling approach especially at higher fluidization velocities.

Several studies on particle mixing in fluidized beds have been presented in the literature (e.g. [3](#)). Suitable validation data on gas and solids mixing in the lower dense part of a CFB is yet sparse. Since similar conditions prevail in a turbulent bed and at the bottom of a CFB, fluidization characteristics as well as gas and solids mixing were studied in this work experimentally in a 2D turbulent bed cold model ([4,5](#)). CFD simulations of the experiments were carried out in 2D and the computational results were compared with the experimental data.

Simulation results for CFBs obtained with standard kinetic theory models have often been poor and the pressure profile far from the measured one (see e.g. [6](#)). Kallio ([7](#)) showed that the computational results can be improved in processes with high fluidization velocities by modifying the standard drag laws of the commercial CFD codes. In the present study, the modified drag model was tested in the case of a turbulent fluidized bed.

MEASUREMENTS OF FLOW PATTERNS AND MIXING IN A TURBULENT FLUIDISED BED

The transparent walls of the turbulent bed cold model are 90 cm wide and 125 cm high. The distance between the walls is 1.5 cm. The air distributor at the bottom consists of 9 orifices with an area of $1.21 \times 1.21 \text{ cm}^2$ each. Three orifices of the same type are placed at a side wall at the heights of 35, 50 and 70 cm. Two fixed bed heights were used in the experiments, 20 and 30 cm. Air flow rates in the experiments were 1250, 1000, 750, 500 and 350 l/min, corresponding to superficial velocities 1.54, 1.23, 0.93, 0.62 and 0.43 m/s, respectively. Bed material density was 2480 kg/m^3 and the mean diameter of the spherical particles $385 \text{ }\mu\text{m}$ (size range $355\text{--}425 \text{ }\mu\text{m}$). Figure 1 shows typical flow patterns at fluidization velocity 1.54 m/s.



Figure 1. Flow structure at air flow rate 1250 l/min ($U=1.54 \text{ m/s}$).

The experiments were recorded on video at 25 Hz and the video images were analyzed by an in-house Visual Basic code. Voidage was determined from the videos by converting the brightness scale into a solids concentration scale. Axial profiles of average solids concentration at the different fluidization conditions are shown in Figure 2. A dense bottom region is found in all cases. Increase in fluidization velocity leads to a decrease in solids concentration at bed bottom.

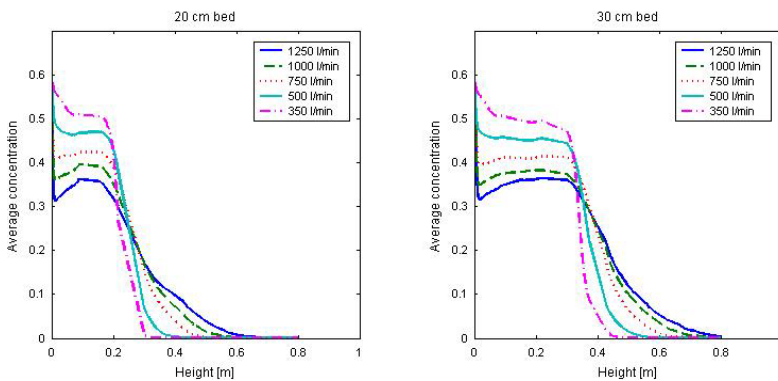


Figure 2. Average solids volume fraction at the different gas velocities for the 20 cm and 30 cm high beds.

Gas mixing studies with CO_2 as tracer were conducted to evaluate the penetration depth of gas jets in the case of the 20 cm fixed bed. A small amount of CO_2 was mixed in air and the gas mixture was blown into the bed at the heights of 35, 50 and 70 cm, either horizontally or downwards at 45 degrees angle. The amount of this secondary gas was 250 l/min. Fluidization velocities 1.54, 1.23 and 0.93 m/s were used in the tests. The concentration of CO_2 was measured at 118 cm height above the bottom plate at 5 cm intervals for 10 s at each measurement location. In addition, some measurements were done at lower elevations through small holes drilled through the walls. Lateral mixing mainly took place at the elevation just (10-20 cm) above the jet entrance level. The main parameter affecting the penetration length of a gas jet was found to be the height at which the jet enters the bed, which is correlated with the local wall layer thickness as well as the suspension density in the

vicinity of the orifice inlet. The fluidization velocity and the gas flow rate through the orifice also affect lateral mixing of gas. These effects are illustrated in Figure 3. The experiments on turbulent fluidization and gas mixing are described in detail in Kallio & Hermanson (4).

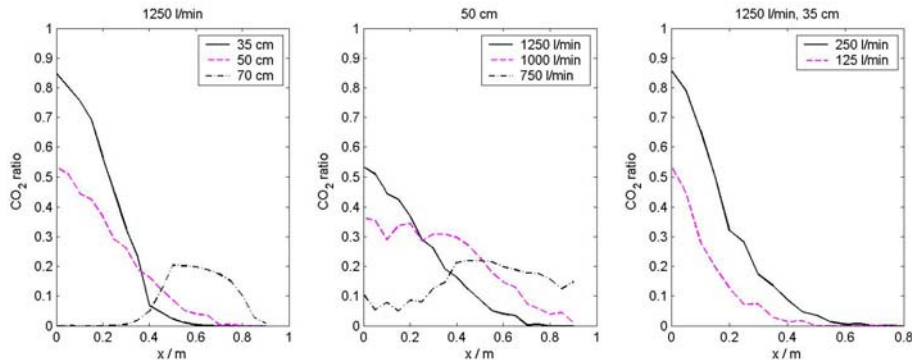


Figure 3. Effects of process parameters on spreading of a gas jet blown through an orifice at a side wall: the effect of the height at which the jet enters the bed (left), the effect of fluidization velocity (middle) and the effect of the gas flow rate through the orifice (right). CO₂ ratio is the ratio of the measured average concentration at 118 cm height to the concentration at the orifice inlet. x is the distance to the side wall.

Experiments were also conducted to gain information on solids mixing (5). Tracer particles were fed through an orifice at 70 cm height on a side wall. The size of the red tracer particles ranged between 0.84 mm and 1.19 mm, and the material density was 1050 kg/m³. The number of particles observed in the left low corner was counted from video recordings (Figure 10).

SIMULATIONS OF TURBULENT FLUIDIZATION

The simulated cases correspond to the experimental arrangement, where the packed bed height was 20 cm and the volumetric air flow rate was 1250 l/min. In the computation, the air was fed to a volume below the grate, from where the air spread into the bed through the nine grate openings with a given pressure drop, see Figure 5. The base turbulent bed and the cases with the secondary air introduced to the bed from the side opening at the heights of 35 cm and 50 cm were simulated. The amount of the secondary air was 250 l/min and the direction either horizontal or 45° downwards. In addition, a case of particle mixing was simulated. The computations for the base turbulent bed were carried out using Fluent 6.1.18 and MFX. The simulations of gas and solids mixing were performed with Fluent 6.2.16.

Two different 2D grids of 12000 and 16000 cells were applied in the simulations. The grid was made denser in the lower part of the bed in order to facilitate smaller grate openings in the model to study the effect of the increase in the air velocity in the grate openings while keeping the volumetric flow constant.

Hydrodynamic models

The computations were mostly performed with the general hydrodynamic models of Fluent (8). For the momentum exchange coefficient, the model of Gidaspow (9) was used and for the kinetic viscosity of the solid phase the model of Gidaspow *et al.*

was applied (9,10). The simulations with Fluent were carried out as turbulent flow using the dispersed $k-\epsilon$ model of Fluent for multiphase flows (8).

In the MFIX simulations, we used the model of Syamlal and O'Brien for the momentum exchange coefficient and the model of Syamlal *et al.* for the kinetic viscosity of the solid phase (11,12). The MFIX computation was carried out as laminar. In order to facilitate a comparison of the simulation results of the codes, the same case was computed also with Fluent applying the same hydrodynamic models and assuming laminar flow.

The standard drag models do not take into account the particle clustering effects. Therefore, the modified model of Kallio (7), was implemented in Fluent. In this model, for very dense suspensions close to minimum fluidization conditions the drag force is calculated from the Ergun equation (13). In more dilute conditions, the same models as used in Poikolainen (14) are utilized in slightly modified forms. The gas-solid exchange coefficient is given in the form

$$K_{sg} = \frac{3}{4} C_D \frac{\epsilon_s \epsilon_g \rho_g |\vec{v}_s - \vec{v}_g|}{d_s} \frac{1}{(v_{sl}/v_t)^2} \quad (1)$$

For dense suspensions the two-phase theory of bubbling beds yields (15):

$$v_{sl}/v_t = \frac{v_{b\infty}}{v_t} \frac{1}{\epsilon_s} \frac{\epsilon_{s,mf} - \epsilon_s}{1 - \epsilon_s} + \frac{U_{mf}}{v_t} \frac{1}{1 - \epsilon_s} \quad (2)$$

For more dilute suspensions, the slip velocity is obtained from an empirical correlation of exponential form (15):

$$v_{sl}/v_t = A \epsilon_g^B \quad (3)$$

The drag law for a single particle is used in extremely dilute gas-solid suspensions. In the computations, gas-solids drag force is thus calculated from a piecemeal function. Interpolation between equations (2) and (3), Ergun equation and single particle drag is done in the model of C_D by means of weight functions assuming that in the more dilute conditions (solids volume fraction up to 20 %) the voidage function (drag force divided by the drag force acting on a single particle in dilute conditions) is independent of the actual slip velocity. The voidage functions for the Gidaspow and modified models are illustrated in Figure 4. In the present work, the applied values for parameters were $A=2.8$, $B=0.17$ and $v_{b\infty}/v_t = 2.2$.

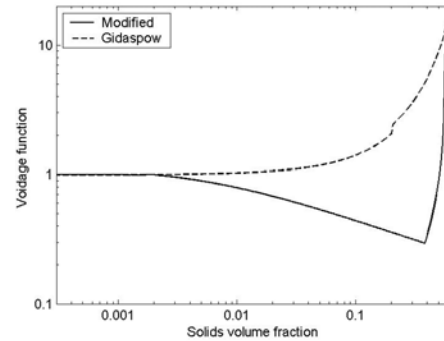


Figure 4. The voidage function used for particle diameter 385 μm , solid density 2480 kg/m^3 , and slip velocity 1 m/s .

FLOW PATTERNS IN THE TURBULENT FLUIDIZED BED

Figure 5 shows typical images of the results for the turbulent bed in three cases. The simulated results are in good agreement with the general understanding of the turbulent fluidised bed behaviour. In the studied cases (bed without the secondary

air through the side opening), the dense areas are found close to the edges of the bed. Inside the bed, the particles form narrow strings and clusters. In the center region of the bed, the clusters are present all the time. The size, location and number of the clusters vary continuously with time due to coalescence and break-up. The strings of the particles splash into the freeboard region above the bed.

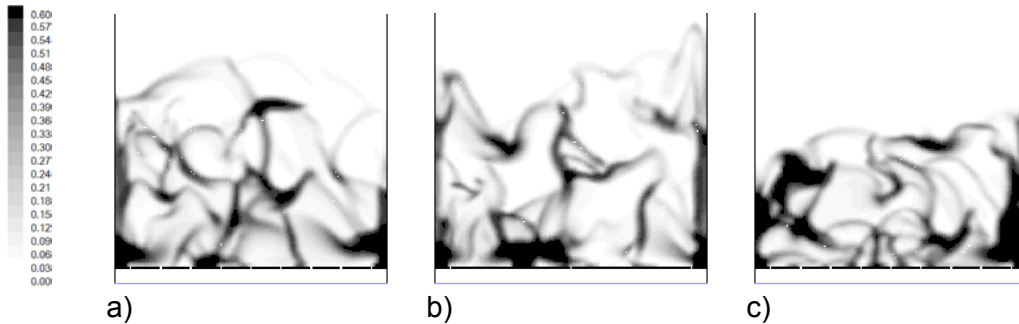


Figure 5. Typical images of the behavior of simulated turbulent bed. From the left: instantaneous volume fraction of particles calculated with a) the Gidaspow models and base grid, b) the denser grid and c) with the modified drag model and base grid.

The measured and computed results were analysed statistically in order to quantify differences. The analyses were performed by calculating the time average of the bed density over a period of 5 seconds. The data was collected every 5 ms. Figure 6 shows the time average of laterally averaged solids volume fractions as a function of bed height. The experimental and computational results with the standard models differ qualitatively. The experimental results indicate a much denser bottom bed than obtained in any of the simulations. On the contrary, the CFD predictions higher up in the bed show a higher particle volume fraction than found in the measurements. The results obtained using the modified drag model are significantly closer to the experimental results. Vertical profiles of the averaged particle volume fractions obtained with the two grid sizes do not differ significantly, as shown in Figure 6. The MFX results are mostly in good agreement with the Fluent results.

Figure 7 shows the simulated and measured lateral profiles of time averaged solids volume fractions at the heights of 20, 40, 60 and 80 cm. The particle concentration at the edges of the upper parts of the bed is clearly greater in the simulation results than in the experimental data. At the bottom of the bed, the difference is opposite.

SIMULATION OF GAS MIXING IN A TURBULENT FLUIDIZED BED

The cases with the secondary air feed were analysed similarly to the base turbulent bed. The secondary air feed seemed to have only a slight effect on the bed behavior independent of the air velocity or direction. This is in accordance with the experimental results which show that the gas penetration depth is quite short and the secondary air restricts to the region neighboring the side opening. The clusters and strings were formed in a same manner as without the secondary air feed.

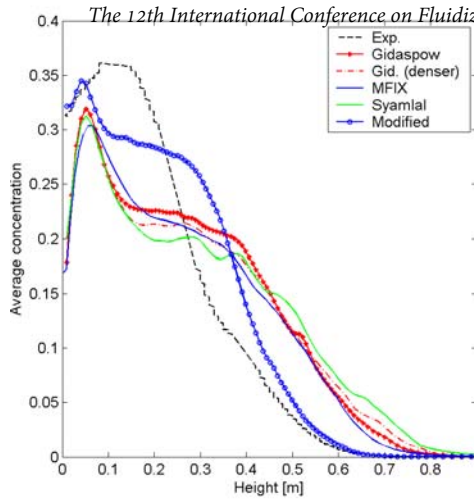


Figure 6. Vertical profiles of the time averaged particle volume fractions for simulated cases and experimental results (see the text for details).

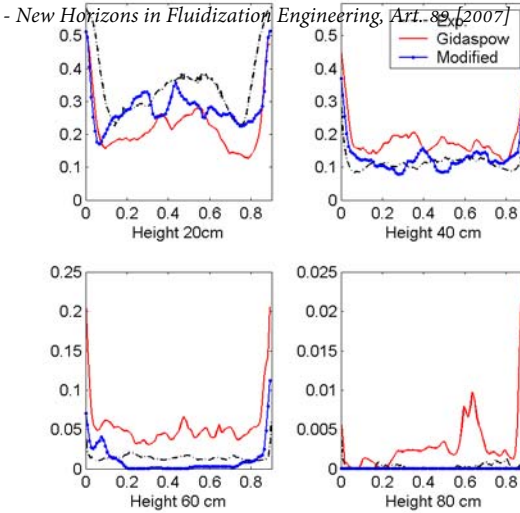


Figure 7. Lateral profiles of the time averaged particle volume fractions for the levels of 20, 40, 60 and 80 cm obtained for the base grid and Gidaspow models, for the modified drag model, and experimental values.

The distribution of the secondary air was studied by adding CO₂ as tracer into the air introduced through the side opening. The CO₂ was modeled as a species in the Fluent 6.2.16 simulations. The inlet concentration of CO₂ was set to 5%. The mixing of the added air was studied by calculating the time average of the concentration of CO₂. The results were compared to the experimental averaged values at the height of 118 cm. The results are shown in Figure 8 for cases with the secondary air inlet at the height of 35 cm and in Figure 9 for cases with the secondary air inlet at the height of 50 cm. The simulations with the horizontal air feed were carried out with both the Gidaspow and modified drag models. The simulation with the air feed directed downwards at 45° angle was carried out only with the Gidaspow model.

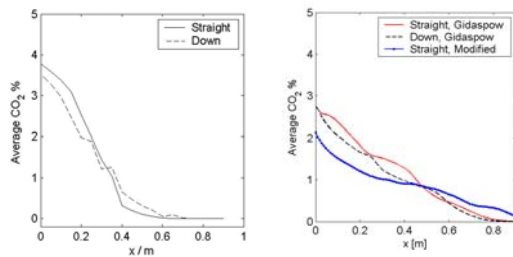


Figure 8. Time averaged lateral concentration of CO₂ at the height of 118 cm, the secondary air inlet at the height 35 cm. On the left: experimental results, on the right: simulated results.

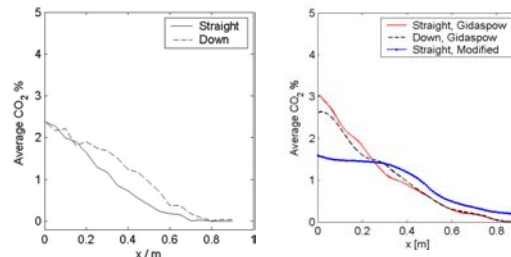


Figure 9. Time averaged lateral concentration CO₂ at the height of 118 cm, the secondary air inlet at the height 50 cm. On the left: experimental results, on the right: simulated results.

Comparing the results in Figures 8 and 9 show that the computational results agree with the measurement data qualitatively. The added air found its way mainly along the edge of the side opening. The migration distance of the added air was longer in

the simulated results than in the experiments. Simulations with the modified drag model resulted in wider spreading of CO₂. The air feed direction has only a slight influence both in the experiments and in the computational results.

SIMULATION OF SOLIDS MIXING IN A TURBULENT FLUIDIZED BED

The experimental case of particle mixing with the fluidization air feed of 1250 l/min was simulated by injecting 4.3 g of additional glass beads with material density of 1050 kg/m³ to a flow domain of a mixed bed in 3 second's period through a side opening at the height of 70 cm. In the experiment, the size of the tracer particles ranged between 0.84 mm and 1.19 mm. In the simulations, an average particle size of 1 mm was used. Both the Gidaspow and modified drag models were utilized. Between the tracer phase and bed particle phase, the symmetric drag model of Syamlal & O'Brien was applied (8).

The mixing of particles was monitored by calculating the number of particles in the region of 17 cm x 12 cm at the bottom corner opposite to the side opening. The number of particles in the monitoring area is represented in Figure 10 as a function of time for both the computation and the experiment. Compared to the experimental results, the simulated large particles entered the monitoring area clearly earlier and the mixing was thus faster.

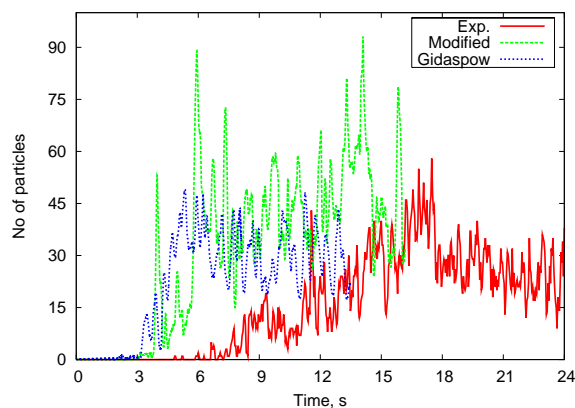


Figure 10. Number of tracer particles in a monitoring area. Results from the simulation and the corresponding experiment are shown.

CONCLUSIONS

The generally accepted hydrodynamic models and a modified drag model were tested for simulation of a turbulent fluidized bed by means of the Eulerian multiphase CFD computations. The validation of the models was based on the experimental results from a 2D turbulent bed. The modified drag model tested in the present work predicts the experimental results at least qualitatively correctly and is easily applicable to small scale processes and phenomena. However, for simulations of large industrial processes, the models still need to be further developed. In such development work, the present models will serve as a good starting point.

ACKNOWLEDGEMENTS

Financial support from Tekes, Neste Oil and Foster Wheeler Energia Oy is gratefully acknowledged.

NOTATION

The 12th International Conference on Fluidization - New Horizons in Fluidization Engineering, Art. 89 [2007]

A, B drag parameters	ε volume fraction [-]
C_D drag coefficient [-]	Subscripts:
d diameter [m]	b^∞ bubble, in infinity
K gas-solid exchange coefficient [$\text{kg/m}^4\text{s}$]	g gas phase
U superficial velocity [m/s]	mf minimum fluidization
v velocity [m/s]	s solid
ρ material density [kg/m^3]	t terminal

REFERENCES

- (1) Gidaspow, D., Jung, J., Singh, R.K., Hydrodynamics of fluidization using kinetic theory: an emerging paradigm: 2002 Flour-Daniel lecture , Review article, Powder Technology, Vol. 148, Issues 2-3, pp. 123-141
- (2) Peirano, E., Modelling and simulation of turbulent gas-solid flows applied to Fluidization, PhD thesis, Chalmers University of Technology, Göteborg, 1998
- (3) Pallarès, D., Johnsson, F., A novel technique for particle tracking in cold 2-dimensional fluidized beds – simulating fuel dispersion, Chem. Eng. Sci. 61, pp. 2710-2720, 2006.
- (4) Kallio, S., Hermanson, A., Experimental study of flow patterns in a 2D turbulent fluidised bed cold model, Åbo Akademi University, Heat Engineering Laboratory, Report 2005-2, 2005.
- (5) Kallio, S., Hermanson, A., Experimental study of solids mixing in a 2D fluidised bed cold model, Åbo Akademi University, Heat Engineering Laboratory, Report 2006-2, 2006.
- (6) Flour, I., Balzer, G., Numerical simulation of the gas-solid flow in the boiler of a 250 MWe CFB plant with ESTET-ASTRID code, Circulating fluidized bed technology VI, Proceedings of the 6th int. conf. on CFBs, Würzburg, Germany, 1999.
- (7) Kallio, S., The role of the gas-solid drag force in CFB modelling of fluidization, Åbo Akademi University, Heat Engineering Laboratory, Report 2005-3, 2005
- (8) Fluent Inc., Fluent Users' guide – Release 6.0, 2001
- (9) Gidaspow, D., Bezburuah, R., Ding., J., Hydrodynamics of circulating fluidized beds, kinetic theory approach. Fluidization VII, Proceedings of the 7th Engineering Foundation Conference on Fluidization, pp. 75-82, 1992.
- (10) Ding, J., Gidaspow, D., A Bubbling fluidization model using kinetic theory of granular flow. AIChE Journal, Vol. 36, No. 4, 1990.
- (11) MFX Documentation, Theory Guide, Technical Note, U.S. Department of energy, 2003, www.mfix.org
- (12) Syamlal, M., Rogers, W., O'Brien, T.J., MFX Documentation, Volume 1, Theory Guide. National Technical Information Service, Springfield, VA, DOE/METC-9411004, NTIS/DE9400087, 1993
- (13) Ergun, S., Fluid flow through packed columns, Chemical Engineering Progress, 48, pp. 89-94, 1952
- (14) Poikolainen, V., Mathematical modelling of gas-solid fluidization with a one-dimensional hydrodynamic model (in Finnish), Lappeenranta university of Technology, Master of Science Thesis, 1992
- (15) Matsen, J.M. Mechanisms of choking and entrainment, Powder Tech. 32, pp. 21-33, 1982